HHS Public Access

Author manuscript

Shock. Author manuscript; available in PMC 2021 August 01.

Published in final edited form as:

Shock. 2020 August ; 54(2): 245–255. doi:10.1097/SHK.0000000000001445.

Critical Role of Mortalin/GRP75 in Endothelial Cell Dysfunction Associated with Acute Lung Injury

Antony Leonard[1], **Pei Yi Su**[1], **David I. Yule**[2], **Arshad Rahman**[1,2], **Fabeha Fazal**[1,2,*]

[1]Department of Pediatrics, Lung Biology and Disease Program, University of Rochester School of Medicine and Dentistry, Rochester, New York 14642

[2]Department of Pharmacology & Physiology, Lung Biology and Disease Program, University of Rochester School of Medicine and Dentistry, Rochester, New York 14642

Abstract

Mortalin/GRP75 (glucose regulated protein 75), a member of heat shock protein 70 (Hsp70) family of chaperones, is involved in several cellular processes including proliferation and signaling, and plays a pivotal role in cancer and neurodegenerative disorders. In this study, we sought to determine the role of mortalin/GRP75 in mediating vascular inflammation and permeability linked to the pathogenesis of acute lung injury (ALI). In an aerosolized bacterial lipopolysaccharide (LPS) inhalation mouse model of ALI, we found that administration of mortalin/GRP75 inhibitor MKT-077, both prophylactically and therapeutically, protected against PMN influx into alveolar airspaces, microvascular leakage and expression of pro-inflammatory mediators such as IL-1β, E-selectin and TNFα. Consistent with this, thrombin-induced inflammation in cultured human endothelial cells (EC) was also protected upon before and after treatment with MKT-077. Similar to pharmacological inhibition of mortalin/GRP75, siRNA-mediated depletion of mortalin/GRP75 also blocked thrombin-induced expression of proinflammatory mediators such as ICAM-1 and VCAM-1. Mechanistic analysis in EC revealed that inactivation of mortalin/GRP75 interfered with the binding of the liberated NF-κB to the DNA, thereby leading to inhibition of downstream expression of adhesion molecules, cytokines and chemokines. Importantly, thrombin-induced Ca^{2+} signaling and EC permeability were also prevented upon mortalin/GRP75 inactivation/depletion. Thus, this study provides evidence for a novel role of mortalin/GRP75 in mediating EC inflammation and permeability associated with ALI.

INTRODUCTION:

Acute lung injury (ALI) and its more severe form acute respiratory syndrome (ARDS) are life-threatening diseases in critically ill patients with a mortality rate between 25–40%. ALI

*Address correspondence and requests to: Fabeha Fazal, Ph.D., Department of Pediatrics, Box 850, Lung Biology and Disease Program, University of Rochester School of Medicine and Dentistry, 601 Elmwood Avenue, Rochester, New York 14642, Phone: (585) 275-5948, Fax: (585) 756-7780, Fabeha_Fazal@URMC.Rochester.edu.

Author contributions: F.F, A.L. and A.R. conceived and designed the experiments. A.L and P.S performed the experiments (equal contribution). F.F analyzed the data and drafted the manuscript. F.F, D.Y and A.R edited and approved the final version of the manuscript.

Conflict of interest: No conflict of interest, financial or otherwise, are declared by the authors

can be precipitated by direct insults such as pneumonia, aspiration or via indirect insults such as sepsis and multiple trauma to the lungs (3). The hallmarks of ALI include severe inflammation (characterized by massive infiltration of polymorphonuclear leukocytes [PMN] into the lung) and disruption of capillary-alveolar barriers resulting in interstitial edema, inflammatory infiltrates, alveolar flooding, and ultimately respiratory failure(16, 20, 38). All current therapies for ALI rely on supportive care and no effective drugs have been developed. Thus, there is an urgent need to develop new treatment strategies for ALI/ARDS that are safe and effective.

Pulmonary endothelium is strategically positioned at the interface between the bloodstream and the lung tissue and is an important component of capillary-alveolar unit. Because of its unique localization it is susceptible to injury from a number of cellular, chemical or mechanical agents that are either inhaled or delivered to the lung through the pulmonary circulation and may cause ALI in animals and humans (19, 26). Upon bacterial infection, component of the gram negative bacterial cell wall such as lipopolysaccharide (LPS) activate pattern recognition receptors on EC, instigating an inflammatory response. This results in induction of a number of host-derived mediators, including cytokines and chemokines, which further stimulate EC to activate NF-κB, a master regulator of inflammation (29). Activated NF-κB renders the otherwise antiadhesive and semipermeable microvasculature into a proadhesive and leaky one (7, 28, 31, 34). NF-κB causes these changes by activating numerous genes including adhesion molecules (E-selectin, ICAM-1, VCAM-1), cytokines (TNFα, IL-1β, IL-6), and chemokines (IL-8, MCP-1*)* (4, 21, 30, 41). The coordinate and concerted action of these proteins serves to facilitate adhesion and transendothelial migration (TEM) of PMN, and to increase endothelial permeability associated with ALI/ ARDS (1, 8, 30, 33).

Mortalin/GRP75 was initially identified in the cytoplasmic fractions of mouse embryonic fibroblasts (MEFs). Later studies revealed its ubiquitous presence in different cell types and in different subcellular localizations (5, 11). In mouse, mortalin (mot) exists in two forms, mot-1 and mot-2; differing only by two amino acids at the carboxy terminus of the protein, but have contrasting functions. Overexpression of mot-1 induced senescence in NIH 3T3 cells, whereas, overexpression of mot-2 promoted malignant phenotype (5, 12, 36, 37). Interestingly, in humans, mot-2 (98% homology to mouse mot-2) is the only transcript expressed and microscopic analyses have shown that it exists in various subcellular sites. Mortalin/GRP75 plays an essential role in mitochondrial import, regulation of mitochondrial membrane potential, intracellular transport, chaperoning, oxidative stress, cellular proliferation and apoptosis (10, 11, 22, 27, 40). Dysfunction of mortalin/GRP75 is associated with several pathological conditions. Parkinson’s and Alzheimer’s are associated with diminished mortalin/GRP75 activity/levels in brain tissues (9, 17, 39), and its reconstitution in these tissues has shown protective effect against neurodegeneration (17, 39). Mortalin/GRP75 is overexpressed in a variety of cancers and contributes to the process of carcinogenesis by multiple mechanisms including inactivation of tumor suppressor p53 protein, deregulation of apoptosis and activation of EMT (epithelial-mesenchymal transition) signaling. MKT-077, a cationic rhodacyanine dye, binds to the nucleotide-binding domain (NBD) of mortalin/GRP75 causing tertiary structural changes resulting in inactivation of the ATPase activity of mortalin/GRP75. Interestingly, MKT-077 only inhibits

the activity of mot-2 and not mot-1 (5). MKT-077 was shown to inhibit growth of several human cancer cell lines and has also shown positive benefits in phase I/II cancer clinical trials (5).

The role of mortalin/GRP75 in ALI, particularly in the context of EC, remains to be addressed. In the present study, we investigated if mortalin/GRP75 is linked to inflammatory and barrier disruptive pathways in the lung endothelium and thereby contributes to ALI. Our data identifies a novel, previously undescribed role of mortalin/GRP75 in the mechanism of EC inflammation and barrier disruption during ALI.

Materials and Methods

Reagents

Human alpha thrombin was obtained from Enzyme Research Laboratories (South Bend, IN). Lipopolysaccharide (LPS – cat # L3129) from *E. coli* and diethylaminoethyl (DEAE)-dextran and MKT-077 were purchased from Sigma-Aldrich Chemical (St. Louis, MO). Polyclonal antibodies to VCAM-1, ICAM-1, IκBα, RelA/p65, GAPDH and β-actin were from Santa Cruz Biotechnology (CA). Control siRNA and siRNA for mortalin/GRP75 were purchased from Dharmacon. Mortalin/GRP75 polyclonal antibody and anti-RelA/p65 (phospho Ser^{536}) antibody were obtained from Cell Signaling Technology (Beverly, MA). All other materials were from VWR Scientific Products Corporation (Gaithersburg, MD) and Fisher Scientific (Pittsburgh, PA).

Murine model of ALI

Male 8- to 10-wk-old wild-type (WT) C57BL/6 mice (Jackson, Bar Harbor, ME) were exposed to an aerosol of saline alone or saline containing *Escherichia coli* LPS (0.5mg/ml, 6ml) for 30 min in a chamber, as described (2). All animal care and treatment procedures were approved by the University of Rochester Committee on Animal Resources and performed in accordance with National Institutes of Health guidelines.

Measurement of lung inflammation and injury

Mouse lung homogenates were prepared in radioimmune precipitation (RIPA) buffer supplemented with protease inhibitor cocktail (Sigma-Aldrich)] as described (2, 6, 13). The levels of TNFα, E-selectin, IL-1β, and albumin in lung tissue and BAL fluids were determined using ELISA kits from R&D Systems (Minneapolis, MN) as described (6, 13). The recruitment of PMN in the lung was determined by monitoring the myeloperoxidase activity in the lung tissues as described (2, 6, 13).

Endothelial cells

Human pulmonary artery endothelial cells (HPAEC) were obtained from Lonza (Walkersville, MD) and cultured in 2% gelatin coated flasks using endothelial basal medium 2 (EBM2) with bullet kit additives (BioWhittaker, Walkersville, MD),as described (6, 7). Experiments were performed in cells up to *passage 6*.

Immunoblotting and immunoprecipitation analysis

After appropriate treatments, cells were lysed in radioimmune precipitation (RIPA) buffer containing 50 mM Tris-HCl, pH 7.4, 150 mM NaCl, 0.25 mM EDTA, pH 8.0, 1% deoxycholic acid, 1% Triton X-100, 5 mM NaF, 1 mM sodium orthovanadate supplemented with complete protease inhibitors (Sigma). For immunoblotting, 10 μg of cell lysates were resolved by SDS-PAGE and transferred onto nitrocellulose (Bio-Rad) or polyvinylidene difluoride membranes, and the residual binding sites on the filters were blocked by incubating with 5% (w/v) nonfat dry milk in TBST (10 mM Tris, pH 8.0, 150 mM NaCl, 0.05% Tween 20) for 1 h at room temperature. The membranes were subsequently incubated overnight at 4° C with the indicated antibodies and developed using an enhanced chemiluminesence (ECL) method as described (7). For immunoprecipitation, cell lysates were prepared in 500 μl of Immunoprecipitation lysis buffer (1% NP-40, 50mM Tris HCl (pH 8.0)) and then subjected to preclearing with 50 μl of protein G MicroBeads (Miltenyi Biotec) for 4 h at 4 °C. The precleared lysate was then subjected to immunoprecipitation by incubating with 0.6–1 μg of appropriate antibody and 50 μl of the protein G MicroBeads at 4 °C overnight with gentle shaking as described. The immunoprecipitates were washed four times with the same volume of ice-cold Immunoprecipitation lysis buffer. The proteins in the immunoprecipitates were extracted from the MicroBeads by applying pre-heated 1X SDS sample buffer and subsequently boiled for 15 min. The extracted proteins were subsequently analyzed by immunoblotting. Blots shown in the result section may have come from the membrane with more samples in various groups.

Reporter gene constructs and luciferase assay

The construct pNF-κB-LUC containing five copies of consensus NF-κB sequences linked to a minimal E1B promoter-luciferase gene was purchased from Stratagene (La Jolla, CA). Reporter gene transfections and luciferase assays were performed essentially as described (2). Briefly, 2.5 μg of DNA was mixed with 50 μg/ml DEAE-dextran in serum-free EBM2, and the resulting mixture was applied onto cells that were 60–80% confluent. 0.125 μg of pTKRLUC plasmid (Promega, Madison, WI) containing *Renilla* luciferase gene driven by the constitutively active thymidine kinase promoter was used to normalize the transfection efficiencies. After 1.5 h, cells were exposed to 10% DMSO in serum-free EBM2 for 4 min and then washed twice with PBS and allowed to grow to confluency in EBM2–10% FBS. After appropriate treatments, cells were lysed in passive reporter lysis buffer (Promega) and cell extracts were assayed for firefly and *Renilla* luciferase activities using dual luciferase reporter assay system (Promega).The data were expressed as a ratio of firefly to *Renilla* luciferase activity.

ELISA

Cytokines (IL-6 and IL-1β) and chemokines (IL-8 and MCP-1) levels in HPAEC culture supernatants were determined using ELISA kits from R&D Systems (Minneapolis, MN) according to the manufacturer's recommendations (2, 13).

Immunofluorescence

HPAEC grown to confluence on 2% gelatin-coated coverslips were subjected to immunofluorescence staining as per the protocol described (7, 13). Polyclonal antibody for Mortalin/GRP75 from Cell Signaling Technology was used to visualize mortalin/GRP75. Nuclei were visualized using Hoechst dye. Following staining the coverslips were rinsed in PBS and mounted on the slide using Vectashield mounting media (Vector Laboratories, Lincolnshire, IL). The images were acquired using an Axio Imager M2m confocal microscope (Zeiss).

Nuclear extract preparation and assessment of RelA/p65 DNA binding

After appropriate treatment, cells were washed twice with ice-cold phosphate-buffered saline and resuspended in 400 μl of buffer A (10 mM HEPES [pH 7.9], 10 mM KCl, 0.1 mM EDTA, 0.1 mM EGTA, 1 mM [DTT], and 0.5 mM PMSF). Twenty minutes later, NP-40 was added to a centrifuged for 1 min at 10,000 rpm at 4 °C to collect the supernatants containing the cytoplasmic proteins. Final concentration of 0.6%, and the samples were The pelleted nuclei were resuspended in 100 μl of buffer B (20 mM HEPES [pH 7.9], 0.4 M NaCl, 1 mM EDTA, 1 mM EGTA, 1 mM DTT, and 1 mM PMSF). After 30 min at 4 °C, lysates were centrifuged for 10 min at 10,000 rpm at 4 °C and supernatants containing the nuclear proteins were collected. The DNA binding activity of RelA/p65 was determined using an ELISA-based transcription factor DNA binding assay kit (Cayman Chemical, Ann Arbor, MI) as described (15).

Endothelial permeability assay

Endothelial permeability was measured using Millipore's *In vitro* Vascular Permeability Assay Kit. HPAEC transfected with control-siRNA or mortalin-siRNA for 48 hours or treated with MKT-077 for 1 h were seeded at 20,000 cells per transwell insert and cultured for 48 h. Following this, the confluent monolayer was treated with thrombin (5 U/ml) for 30 minutes. FITC-Dextran permeability testing was done to check monolayer integrity. Permeation was stopped by removing the inserts from the wells. Media from the receiver tray was transferred to a 96 well opaque plate to measure fluorescence. Fluorescent intensities were quantified using a fluorescent plate reader with filters appropriate for 485 nm and 535 nm excitation and emission. The endothelial monolayer was stained to check for monolayer integrity using Cell Stain provided in the kit (14). Cells were visualized using the Leica DMI 3000B fluorescent microscope.

Cytosolic Ca^{2+} measurements in intact cell population

HPAEC grown to confluence on 25mm glass coverslips (Fisher Scientific) were loaded with 2μM Fura-2 AM (Invitrogen), a cell permeable fluorescent probe used for measuring change in cytosolic Ca^{2+}, for 30 minutes. After dye loading, the cells were washed twice with Ca^{2+} free HBSS buffer, and the coverslips were mounted on an inverted microscope (Eclipse TE2000-E, Nikon). Calcium release from the intracellular stores was determined by perfusing Ca^{2+} free imaging buffer and stimulating cells with thrombin (2.5U). Store-operated Ca^{2+} entry was measured, following addition of 1.26 mM Ca^{2+}. Images were captured at 510nm using a digital CCD camera (CoolSNAP HQ2, Photometrics) and an

imaging software (NIS-Element AR 3.0, Nikon) after alternating excitations at 340 and 380nm. Fura-2 ratio (F-ratio 340/380) was calculated and analyzed later offline with NIS-Element AR 3.0 Software (13).

Arterial oxygen saturation measurements:

The MouseOx™ Pulse-oximeter (Starr Life Sciences, Oakmont PA) is a non-invasive procedure used to measure blood SpO_2 in conscious mice after treatment. Mice were held by hand and the pulse-oximeter clip with Nair (hair removal cream) was placed on the area surrounding the neck to remove the hairs so as to obtain 100% oxygen saturation measurement in mice. Mice were held and covered by the light blocker fabric supplied by the manufacturer and held until calm (several seconds), before placing the probe on the area surrounding the neck. Three-to-five minute readings were taken from each mouse.

Statistical analysis

Standard one-way ANOVA was used to analyze the results, which were presented as mean ± SE. Tukey's test (Prism 5.0, GraphPad Software, San Diego) was used to determine the significance between the groups. A P value <0.05 between two groups was considered statistically significant (2).

RESULTS:

Mortalin/GRP75 is a critical mediator of lung inflammation and injury in mice

Preventive ability and therapeutic potential of mortalin/GRP75 inhibitor MKT-077 was tested in aerosolized bacterial LPS inhalation mouse model of ALI. Wild type C57BL/6L mice were injected i.p. with MKT-077 prior to and after aerosolizing the mice with *E.coli* LPS. LPS inhalation induced significant PMN recruitment into the lung; however, this response was attenuated by MKT-077 in both protective (P) and therapeutic (T) groups (Fig. 1A). Similarly, LPS-induced lung vascular injury was also protected upon therapeutic and prophylactic administration of MKT-077, as evidenced by a marked decrease in albumin level in BALF (bronchoalveolar lavage fluid) (Fig. 1B). LPS-induced levels of proinflammatory mediators such as IL-1β, TNFα and E-selectin were also significantly decreased in the lungs of mice treated with MKT-077 before and after LPS inhalation (Fig.1C–E). These data led us to determine if MKT-077 is also effective in improving lung function in mice challenged with LPS. To this end, we assessed PaO_2 (partial pressure of oxygen) as a measure of lung function in live mice and found that LPS-induced decrease in PaO_2 was protected in mice pretreated with MKT-077 (Fig. 1F&G). Furthermore, since mortalin/GRP75 seems to be a critical player in mediating lung vascular inflammation and injury we also determined if mortalin/GRP75 expression was regulated by LPS-inhalation in mouse model of ALI. No change in the expression of mortalin was observed in lung homogenates of mice treated with LPS (Fig. 1H). Together, these data show that inactivation of mortalin/GRP75 was effective both prophylactically and therapeutically in protecting against LPS-induced lung inflammatory injury in mice.

Mortalin/GRP75 is a critical mediator of EC inflammation

We determined the role of the mortalin/GRP75 in EC inflammation, either by inactivating mortalin using MKT-077 or by depleting mortalin/GRP75 using siRNA. EC treated with MKT-077 before stimulation with thrombin, an edemagenic and proinflammatory agonist, showed a marked decrease in ICAM-1, VCAM-1 and MCP-1 levels as compared to cells treated with thrombin alone (Fig. 2A&B). In addition, pretreatment of EC with MKT-077 blocked both the synthesis and release of thrombin-induced IL-6, as observed by a decrease in IL-6 levels in cell lysate and culture supernatant respectively (Fig. 2C&D). Furthermore, EC treated with MKT-077 before or after stimulation with thrombin, showed a significant reduction in NF-κB transcriptional activity (Fig. 2E). Consistent with this, a reduction in IL-6 and ICAM-1 levels was noted under these conditions (Fig. 2F&G). Similar to thrombin, LPS-induced expression of proinflammatory mediators such as IL-6, ICAM-1 and VCAM-1 were also significantly decreased in the presence of MKT-077 in EC (Fig. 2H&I). Thus, our *in vitro* data mimics our *in vivo* data and reinforces the therapeutic and preventive potential of MKT-077 against LPS-induced inflammatory responses associated with ALI. In the second approach, mortalin was depleted using siRNA. Results indicate a marked reduction (90%) in mortalin protein level in the presence of mortalin siRNA as compared to the cells transfected with control siRNA (Fig. 3A&B). Consistent with the effect of MKT-077 on EC inflammation, depletion of mortalin via siRNA significantly decreased thrombin-induced NF-κB transcriptional activity and resultant adhesion molecules expression (Fig. 3C–F). Together our data establish a crucial role of mortalin/GRP75 in mediating EC inflammation induced by two clinically relevant agonists such as thrombin and LPS.

Mortalin/GRP75 mediates thrombin-induced EC inflammation by regulating NF-κB binding to DNA

Next we analyzed the mechanism by which mortalin/GRP75 regulates NF-κB activity in EC. Phosphorylation of IκBα and its subsequent degradation is a requirement for the release and translocation of RelA/p65 to the nucleus and Ser^{536} phosphorylation of RelA/p65 contributes to its transactivating potential. Hence, MKT-077-treated and mortalin-depleted cells were evaluated for thrombin-induced IκBα degradation, Ser^{536} phosphorylation and RelA/p65 nuclear translocation. We observed that thrombin-induced IκBα degradation, Ser^{536} phosphorylation and RelA/p65 nuclear translocation remained unaffected by inactivation of mortalin (Fig. 4A–C) or depletion of mortalin (Fig. 4D–F). Interestingly, however, thrombin-induced binding of the released RelA/p65 to the DNA was blocked upon inactivation of mortalin by MKT-077 (Fig. 4G). The impaired binding of RelA/p65 to the DNA following MKT-077 treatment prompted us to examine whether RelA/p65 associates with mortalin/GRP75 to facilitate RelA/p65 DNA binding and whether this association is disrupted by MKT-077. Co-immunoprecipitation studies were performed by immunoprecipitating mortalin/GRP75 from control and thrombin treated cells in the presence and absence of MKT077, and the immunoprecipitates were immunoblotted for RelA/p65 (Fig. 4H). In reciprocal experiments RelA/p65 was immunoprecipitated from cells treated with thrombin in the presence and absence of MKT077, and the immunoprecipitates were immunoblotted using anti-mortalin/GRP75 antibody (Fig. 4I). These results indicate that mortalin associates with RelA/p65 irrespective of its inactivation by MKT-077 and also the association is independent of thrombin. Since inactivation of mortalin/GRP75 by

MKT-077 only blocks the binding of released RelA/p65 to DNA and not any of the preceding steps in the NF-κB canonical pathway, it is likely that "active" mortalin/GRP75 bound to RelA/p65 is critical for recruiting coactivators and dissociating HDACs and thereby inducing chromatin remodeling to facilitate RelA/p65 DNA binding. However, this possibility remains to be addressed.

Mortalin/GRP75 is critical to thrombin-induced EC permeability

Disruption of endothelial barrier integrity is a major pathogenic feature of ALI. Hence, we evaluated the role of mortalin/GRP75 in thrombin-induced EC permeability using an *in vitro* permeability assay kit. To this end, EC were transfected with mortalin-siRNA or control-siRNA and were seeded at 20,000 cells per well into transwell inserts and cultured for 48 hours. The confluent monolayer was then treated with thrombin (5 U/ml) for 30 minutes, followed by addition of a high molecular weight FITC-Dextran to monitor EC barrier integrity of permeability. Our results show that knockdown of mortalin significantly reduced thrombin-induced permeability, as indicated by a marked decrease in the fluorescent counts (Fig. 5A). Next the endothelial monolayer was stained to monitor monolayer integrity using Cell stain provided in the kit. Data show that knockdown of mortalin/GRP75 significantly reduced the gaps between untreated and thrombin-treated cells, implying the role of mortalin/GRP75 in EC barrier integrity (Fig. 5B). We also determined the protective and therapeutic effect of mortalin/GRP75 inactivation on thrombin-induced EC permeability. Our data indicated a marked decrease in thrombin-induced permeability in cells treated with MKT-077 either before or after thrombin challenge (Fig. 5C). These data indicates the role of mortalin/GRP75 in regulating thrombin-induced EC barrier disruption.

Mortalin/GRP75 is critical to thrombin-induced Ca^{2+} signaling in EC

In order to explore the mechanism of thrombin-induced EC permeability, we determined the role of mortalin/GRP75 in mediating Ca^{2+} signaling, a critical determinant of EC permeability. HPAEC were pretreated with MKT-077 and then loaded with Fura2-AM for 15 min. Ratiometric measurements of intracellular Ca^{2+} were made in response to thrombin during extracellular Ca^{2+} depletion-repletion conditions. Results indicate that inactivation of mortalin/GRP75 by MKT-077 significantly (50%) blocked the Ca^{2+} release from the ER stores (indicated by the first peak) and also the store-operated Ca^{2+} entry from the extracellular medium (represented by 2^{nd} peak) (Fig.6A&B). Together, these data points to a novel role of mortalin/GRP75 in the mechanism of Ca^{2+} release and entry.

Discussion

In the present study, we have identified a novel role of mortalin/GRP75 in mediating inflammation and permeability linked to the pathogenesis of ALI. Using bacterial LPS inhalation mouse model of ALI, we have shown that administration of mortalin/GRP75 inhibitor MKT-077, either prophylactically or therapeutically, blocked LPS-induced expression of proinflammatory mediators and PMN infiltration into the lungs. MKT-077 also showed protective and therapeutic effect against LPS-induced lung vascular leak. As expected, MKT-077 improved lung function by protecting LPS-induced decrease in PaO_2. Consistent with these findings, our *in vitro* data revealed that inactivation of mortalin by

MKT-077 (both prophylactically and therapeutically) or its depletion using mortalin siRNA blocked thrombin-induced NF-κB activation and proinflammatory gene expression. Further, mechanistic analysis revealed that MKT-077 blocked EC inflammation by inhibiting the binding of the released RelA/p65 to the DNA. In addition, inactivation or depletion of mortalin/GRP75 interfered with thrombin-induced Ca^{2+} signaling and endothelial barrier disruption. Collectively, our *in vivo* and *in vitro* data indicate that mortalin/GRP75 contributes to ALI pathogenesis, at least in part, through its ability to induce EC inflammation and permeability.

Mortalin/GRP75 has been widely studied in the context of neurological disorders and tumorigenesis, diseases with an inflammatory underpinning. Here, we investigated the role of mortalin/GRP75 in lung vascular inflammation and injury. ALI is characterized by three stages that overlap temporally and spatially. The initial stage or the exudative stage involve a complex interaction of inflammation, loss of cellular integrity (destruction of epithelial and endothelial barrier) resulting in flooding of the alveoli with proteinaceous edema fluid and activation of coagulation. The second stage or the recovery phase involves proliferation of epithelial cells, endothelial cells, and fibroblasts. However, in the absence of recovery the lung may progress into the third stage called the fibrotic stage which is characterized by diffuse fibrosis and changes in lung structure (3). In LPS inhalation mouse model of ALI our studies focuses mainly on the initial stage where lung endothelium becomes inflamed and leaky, leading to increased microvascular permeability and generation of protein-rich pulmonary edema(25). Our data show that in addition to IL-1β and TNFα, LPS inhalation induced the expression of E-selectin, which is exclusively expressed on endothelial cell surface and is involved in leukocyte-endothelial adhesion and its elevated level is associated with ALI (24). Intraperitoneal injection of mortalin/GRP75 inhibitor MKT-077 before and after LPS inhalation significantly blocked the inflammatory responses. Similarly, exposure of cultured EC to MKT-077 either before or after thrombin treatment also protected against inflammatory outputs. These observations suggest a crucial role of mortalin/GPR75 in mediating EC inflammation associated with ALI.

Majority of the earlier studies have focused on the role of mortalin in cancer cells and have shown that overexpression of mortalin was sufficient to increase the malignancy of breast cancer cells in both *in vitro* and *in vivo* models (18). The underlying mechanism for the above response was shown to be the sequestration of wild-type p53 with mortalin in the cytoplasm, leading to inhibition of its transcriptional activation and control of centrosome duplication functions. Treatment of cancer cells with MKT-077 releases p53 from mortalin–p53 complex and cause activation of p53 and growth arrest of cancer cells. Along similar lines, mechanistic analysis in our studies showed that mortalin also forms a complex with NF-κB in endothelial cells; interestingly, however, pretreatment with MKT-077 does not release NF-κB from mortalin-NF-κB complex but inhibits the binding of NF-κB to the DNA leading to the inhibition of proinflammatory gene expression. This is the first report showing the role of mortalin/GRP75 in mediating endothelial cell inflammation via regulation of NF-κB. Contrary to our observation in EC, studies in microglial BV-2 cells showed that overexpression of mortalin/GRP75 attenuates LPS-induced oxidative and metabolic responses, and suppresses proinflammatory activation, which depends on NF-κB

activation and lactate generation (35). Thus, mortalin/GRP75 appears to differentially regulate NF-κB depending upon the cellular context.

Furthermore, our studies in EC and in mice highlighted a role of mortalin/GRP75 in mediating vascular barrier disruption. Both therapeutic and prophylactic delivery of MKT-077 prevented thrombin-and LPS-induced barrier dysfunction *in vitro* and *in vivo* respectively. Mechanistic analysis in EC revealed that mortalin contributes to thrombin-induced EC permeability via activation of Ca^{2+} signaling. Thrombin binds to protease activated receptor-1 (PAR1) and activates heterotrimeric G proteins, G_{12}/G_{13} and G_q leading to the generation of inositol 1,4,5-trisphosphate (IP_3), which in turn binds to inositol 1,4,5-trisphosphate receptor (IP_3R) on ER, signaling the release of Ca^{2+} from ER stores. The depletion of Ca^{2+} from the ER induces activation of store-operated channels (SOC) at the plasma membrane, resulting in Ca^{2+} entry from the outside and refilling of ER stores (23). Our data show that pretreatment of HPAEC with MKT-077 decreased both Ca^{2+} release from the ER and subsequent store-depletion operated Ca^{2+} entry (SOCE) from the extracellular milieu in response to thrombin, thereby indicating a role of mortalin/GRP75 in the mechanism of Ca^{2+} release and entry. In addition, studies have shown that caveolin-1-eNOS-dependent NO-redox signaling regulates adherens junction (AJ) disassembly, a critical determinant of EC permeability (32). Our preliminary experiments indicate a decrease in thrombin-induced eNOS phosphorylation at serine 1177 in the presence of MKT-077 (Leonard et al, unpublished data). Comprehensive understanding of the role of mortalin in caveolin-1/eNOS/p190RhoGAP-A pathway regulating EC permeability and its relevance in lung vascular injury will require additional studies using mice with cell specific deletion of mortalin/GRP75.

Together, our data identifies a novel role of mot −2 isoform of mortalin/GRP75 (since MKT-077 specifically inhibits mot-2 and not mot-1) in mediating EC inflammation and permeability associated with ALI in mice. Interestingly, mot-2 is the only isoform of mortalin/GRP75 present in humans; hence these findings enhance the translational significance of mot-2. Overall, the beneficial effect of MKT-077 both prophylactically and therapeutically in controlling ALI, identifies it as a viable therapeutic target.

Acknowledgement:

This work was supported by National Heart Lung and Blood Institute grants HL130870, GM130463 and HL116632. This work was also supported in part by National Institute of Environmental Health Sciences Center (EHSC) Grant ES-01247.

References

1. Basit A, Reutershan J, Morris MA, Solga M, Rose CE Jr., and Ley K. ICAM-1 and LFA-1 play critical roles in LPS-induced neutrophil recruitment into the alveolar space. Am J Physiol Lung Cell Mol Physiol 291: L200–207, 2006. [PubMed: 16461431]
2. Bijli KM, Fazal F, Slavin SA, Leonard A, Grose V, Alexander WB, Smrcka AV, and Rahman A. Phospholipase C-epsilon signaling mediates endothelial cell inflammation and barrier disruption in acute lung injury. Am J Physiol Lung Cell Mol Physiol 311: L517–524, 2016. [PubMed: 27371732]
3. Cross LJ and Matthay MA. Biomarkers in acute lung injury: insights into the pathogenesis of acute lung injury. Critical care clinics 27: 355–377, 2011. [PubMed: 21440206]

4. Dagia NM, Agarwal G, Kamath DV, Chetrapal-Kunwar A, Gupte RD, Jadhav MG, Dadarkar SS, Trivedi J, Kulkarni-Almeida AA, Kharas F, Fonseca LC, Kumar S, and Bhonde MR. A preferential p110alpha/gamma PI3K inhibitor attenuates experimental inflammation by suppressing the production of proinflammatory mediators in a NF-kappaB-dependent manner. Am J Physiol Cell Physiol 298: C929–941, 2010. [PubMed: 20089935]
5. Deocaris CC, Lu WJ, Kaul SC, and Wadhwa R. Druggability of mortalin for cancer and neuro-degenerative disorders. Current pharmaceutical design 19: 418–429, 2013. [PubMed: 22920904]
6. Fazal F, Bijli KM, Murrill M, Leonard A, Minhajuddin M, Anwar KN, Finkelstein JN, Watterson DM, and Rahman A. Critical role of non-muscle myosin light chain kinase in thrombin-induced endothelial cell inflammation and lung PMN infiltration. PloS one 8: e59965, 2013. [PubMed: 23555849]
7. Fazal F, Minhajuddin M, Bijli KM, McGrath JL, and Rahman A. Evidence for actin cytoskeleton-dependent and -independent pathways for RelA/p65 nuclear translocation in endothelial cells. J Biol Chem 282: 3940–3950, 2007. [PubMed: 17158457]
8. Gao X, Xu N, Sekosan M, Mehta D, Ma SY, Rahman A, and Malik AB. Differential role of CD18 integrins in mediating lung neutrophil sequestration and increased microvascular permeability induced by Escherichia coli in mice. J Immunol 167: 2895–2901, 2001. [PubMed: 11509637]
9. Jin J, Hulette C, Wang Y, Zhang T, Pan C, Wadhwa R, and Zhang J. Proteomic identification of a stress protein, mortalin/mthsp70/GRP75: relevance to Parkinson disease. Molecular & cellular proteomics : MCP 5: 1193–1204, 2006. [PubMed: 16565515]
10. Johnson RF, Witzel II, and Perkins ND. p53-dependent regulation of mitochondrial energy production by the RelA subunit of NF-kappaB. Cancer research 71: 5588–5597, 2011. [PubMed: 21742773]
11. Kaul SC, Deocaris CC, and Wadhwa R. Three faces of mortalin: a housekeeper, guardian and killer. Experimental gerontology 42: 263–274, 2007. [PubMed: 17188442]
12. Kaul SC, Duncan E, Sugihara T, Reddel RR, Mitsui Y, and Wadhwa R. Structurally and functionally distinct mouse hsp70 family members Mot-1 and Mot-2 proteins are encoded by two alleles. DNA research : an international journal for rapid publication of reports on genes and genomes 7: 229–231, 2000. [PubMed: 10907855]
13. Leonard A, Grose V, Paton AW, Paton JC, Yule DI, Rahman A, and Fazal F. Selective Inactivation of Intracellular BiP/GRP78 Attenuates Endothelial Inflammation and Permeability in Acute Lung Injury. Scientific reports 9: 2096, 2019. [PubMed: 30765717]
14. Leonard A, Paton AW, El-Quadi M, Paton JC, and Fazal F. Preconditioning with endoplasmic reticulum stress ameliorates endothelial cell inflammation. PloS one 9: e110949, 2014. [PubMed: 25356743]
15. Leonard A, Rahman A, and Fazal F. Importins alpha and beta signaling mediates endothelial cell inflammation and barrier disruption. Cellular signalling 44: 103–117, 2018. [PubMed: 29331583]
16. Levitt JE and Matthay MA. Treatment of acute lung injury: historical perspective and potential future therapies. Seminars in respiratory and critical care medicine 27: 426–437, 2006. [PubMed: 16909376]
17. Liu Y, Liu W, Song XD, and Zuo J. Effect of GRP75/mthsp70/PBP74/mortalin overexpression on intracellular ATP level, mitochondrial membrane potential and ROS accumulation following glucose deprivation in PC12 cells. Molecular and cellular biochemistry 268: 45–51, 2005. [PubMed: 15724436]
18. Lu WJ, Lee NP, Kaul SC, Lan F, Poon RT, Wadhwa R, and Luk JM. Mortalin-p53 interaction in cancer cells is stress dependent and constitutes a selective target for cancer therapy. Cell death and differentiation 18: 1046–1056, 2011. [PubMed: 21233847]
19. Maniatis NA, Kotanidou A, Catravas JD, and Orfanos SE. Endothelial pathomechanisms in acute lung injury. Vascul Pharmacol 49: 119–133, 2008. [PubMed: 18722553]
20. Matthay MA and Zimmerman GA. Acute lung injury and the acute respiratory distress syndrome: four decades of inquiry into pathogenesis and rational management. Am J Respir Cell Mol Biol 33: 319–327, 2005. [PubMed: 16172252]

21. Meng F, Meliton A, Moldobaeva N, Mutlu G, Kawasaki Y, Akiyama T, and Birukova AA. Asef mediates HGF protective effects against LPS-induced lung injury and endothelial barrier dysfunction. Am J Physiol Lung Cell Mol Physiol 308: L452–463, 2015. [PubMed: 25539852]
22. Moro F, Okamoto K, Donzeau M, Neupert W, and Brunner M. Mitochondrial protein import: molecular basis of the ATP-dependent interaction of MtHsp70 with Tim44. J Biol Chem 277: 6874–6880, 2002. [PubMed: 11733493]
23. Nilius B and Droogmans G. Ion channels and their functional role in vascular endothelium. Physiol Rev 81: 1415–1459, 2001. [PubMed: 11581493]
24. Okajima K, Harada N, Sakurai G, Soga Y, Suga H, Terada T, and Nakagawa T. Rapid assay for plasma soluble E-selectin predicts the development of acute respiratory distress syndrome in patients with systemic inflammatory response syndrome. Translational research : the journal of laboratory and clinical medicine 148: 295–300, 2006. [PubMed: 17162250]
25. Olman MA, White KE, Ware LB, Simmons WL, Benveniste EN, Zhu S, Pugin J, and Matthay MA. Pulmonary edema fluid from patients with early lung injury stimulates fibroblast proliferation through IL-1 beta-induced IL-6 expression. J Immunol 172: 2668–2677, 2004. [PubMed: 14764742]
26. Orfanos SE, Mavrommati I, Korovesi I, and Roussos C. Pulmonary endothelium in acute lung injury: from basic science to the critically ill. Intensive care medicine 30: 1702–1714, 2004. [PubMed: 15258728]
27. Park SJ, Shin JH, Jeong JI, Song JH, Jo YK, Kim ES, Lee EH, Hwang JJ, Lee EK, Chung SJ, et al. Down-regulation of mortalin exacerbates Abeta-mediated mitochondrial fragmentation and dysfunction. J Biol Chem 289: 2195–2204, 2014. [PubMed: 24324263]
28. Rahman A, Anwar KN, Uddin S, Xu N, Ye RD, Platanias LC, and Malik AB. Protein kinase C-delta regulates thrombin-induced ICAM-1 gene expression in endothelial cells via activation of p38 mitogen-activated protein kinase. Mol Cell Biol 21: 5554–5565, 2001. [PubMed: 11463837]
29. Rahman A and Fazal F. Blocking NF-kappaB: an inflammatory issue. Proceedings of the American Thoracic Society 8: 497–503, 2011. [PubMed: 22052926]
30. Rahman A and Fazal F. Hug tightly and say goodbye: role of endothelial ICAM-1 in leukocyte transmigration. Antioxid Redox Signal 11: 823–839, 2009. [PubMed: 18808323]
31. Rahman A, True AL, Anwar KN, Ye RD, Voyno-Yasenetskaya TA, and Malik AB. Galpha(q) and Gbetagamma regulate PAR-1 signaling of thrombin-induced NF-kappaB activation and ICAM-1 transcription in endothelial cells. Circ Res 91: 398–405, 2002. [PubMed: 12215488]
32. Siddiqui MR, Komarova YA, Vogel SM, Gao X, Bonini MG, Rajasingh J, Zhao YY, Brovkovych V, and Malik AB. Caveolin-1-eNOS signaling promotes p190RhoGAP-A nitration and endothelial permeability. J Cell Biol 193: 841–850, 2011. [PubMed: 21624953]
33. Springer TA. Traffic signals for lymphocyte recirculation and leukocyte emigration: the multistep paradigm. Cell 76: 301–314, 1994. [PubMed: 7507411]
34. Tiruppathi C, Shimizu J, Miyawaki-Shimizu K, Vogel SM, Bair AM, Minshall RD, Predescu D, and Malik AB. Role of NF-kappaB-dependent caveolin-1 expression in the mechanism of increased endothelial permeability induced by lipopolysaccharide. J Biol Chem 283: 4210–4218, 2008. [PubMed: 18077459]
35. Voloboueva LA, Emery JF, Sun X, and Giffard RG. Inflammatory response of microglial BV-2 cells includes a glycolytic shift and is modulated by mitochondrial glucose-regulated protein 75/mortalin. FEBS letters 587: 756–762, 2013. [PubMed: 23395614]
36. Wadhwa R, Kaul SC, Mitsui Y, and Sugimoto Y. Differential subcellular distribution of mortalin in mortal and immortal mouse and human fibroblasts. Exp Cell Res 207: 442–448, 1993. [PubMed: 8344392]
37. Wadhwa R, Kaul SC, Sugimoto Y, and Mitsui Y. Induction of cellular senescence by transfection of cytosolic mortalin cDNA in NIH 3T3 cells. J Biol Chem 268: 22239–22242, 1993. [PubMed: 7693662]
38. Ware LB and Matthay MA. The acute respiratory distress syndrome. The New England journal of medicine 342: 1334–1349, 2000. [PubMed: 10793167]
39. Xu L, Voloboueva LA, Ouyang Y, Emery JF, and Giffard RG. Overexpression of mitochondrial Hsp70/Hsp75 in rat brain protects mitochondria, reduces oxidative stress, and protects from focal

ischemia. Journal of cerebral blood flow and metabolism : official journal of the International Society of Cerebral Blood Flow and Metabolism 29: 365–374, 2009.

40. Yaguchi T, Aida S, Kaul SC, and Wadhwa R. Involvement of mortalin in cellular senescence from the perspective of its mitochondrial import, chaperone, and oxidative stress management functions. Annals of the New York Academy of Sciences 1100: 306–311, 2007. [PubMed: 17460192]
41. You J, Peng W, Lin X, Huang QL, and Lin JY. PLC/CAMK IV-NF-kappaB involved in the receptor for advanced glycation end products mediated signaling pathway in human endothelial cells. Molecular and cellular endocrinology 320: 111–117, 2010. [PubMed: 20171262]

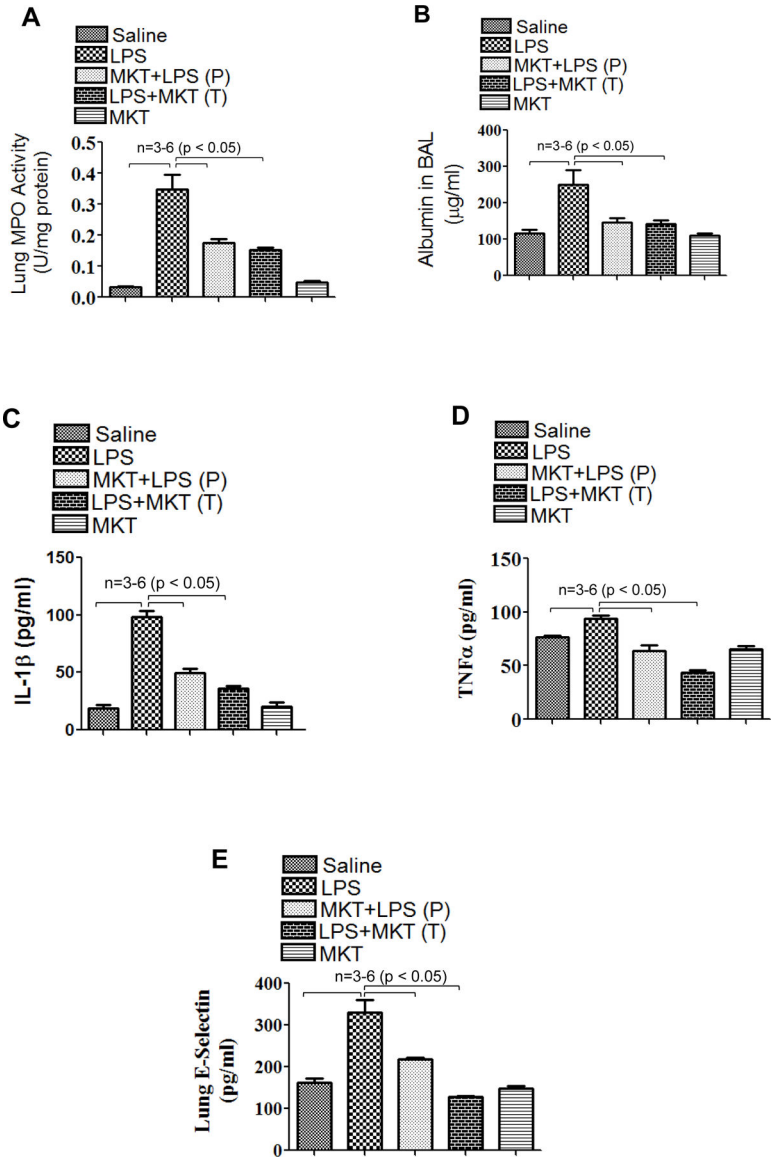

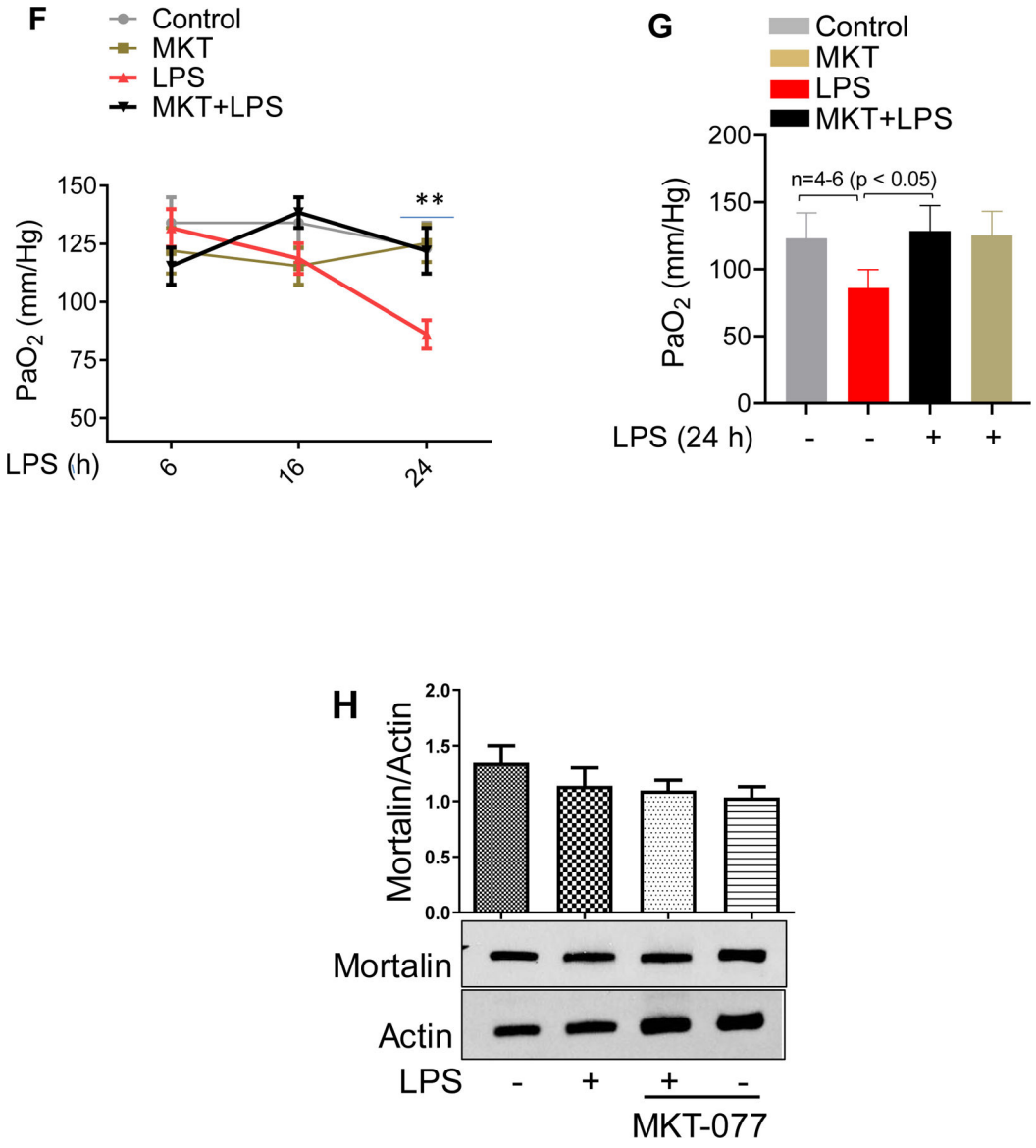

Figure 1. MKT-077 protects against LPS-induced lung inflammation and injury.

Wild type C57BL/6L mice were injected i.p. with MKT-077 (5 mg/kg) 1 h prior to or 1 h after aerosolizing the mice with E. coli LPS (0.5mg/ml; 6ml) for 30 min. Mice injected i.p. with saline 1 h prior to aerosolization served as control. After 16 h, lung homogenates were analyzed for ***(A)*** MPO activity, ***(C)*** IL-1β, ***(D)*** TNFα, ***(E)*** E-selectin and BAL fluid was analyzed for ***(B)*** albumin. Wild type C57BL/6L mice were injected i.p. with MKT-077 (5 mg/kg) 1 h prior to aerosolizing the mice with E. coli LPS (0.5mg/ml; 6ml) for 30 min. Six, sixteen and twenty four hours post LPS challenge, PaO_2 was measured using MouseOx™ Pulse-oximeter as described in Methods ***(F&G).*** Wild type C57BL/6L mice were injected i.p. with MKT-077 (5 mg/kg) 1 h prior to aerosolizing the mice with E. coli LPS (0.5mg/ml; 6ml) for 30 min. After 16 h, lung homogenates were analyzed for levels of mortalin ***(H).*** Actin was used as a loading control.

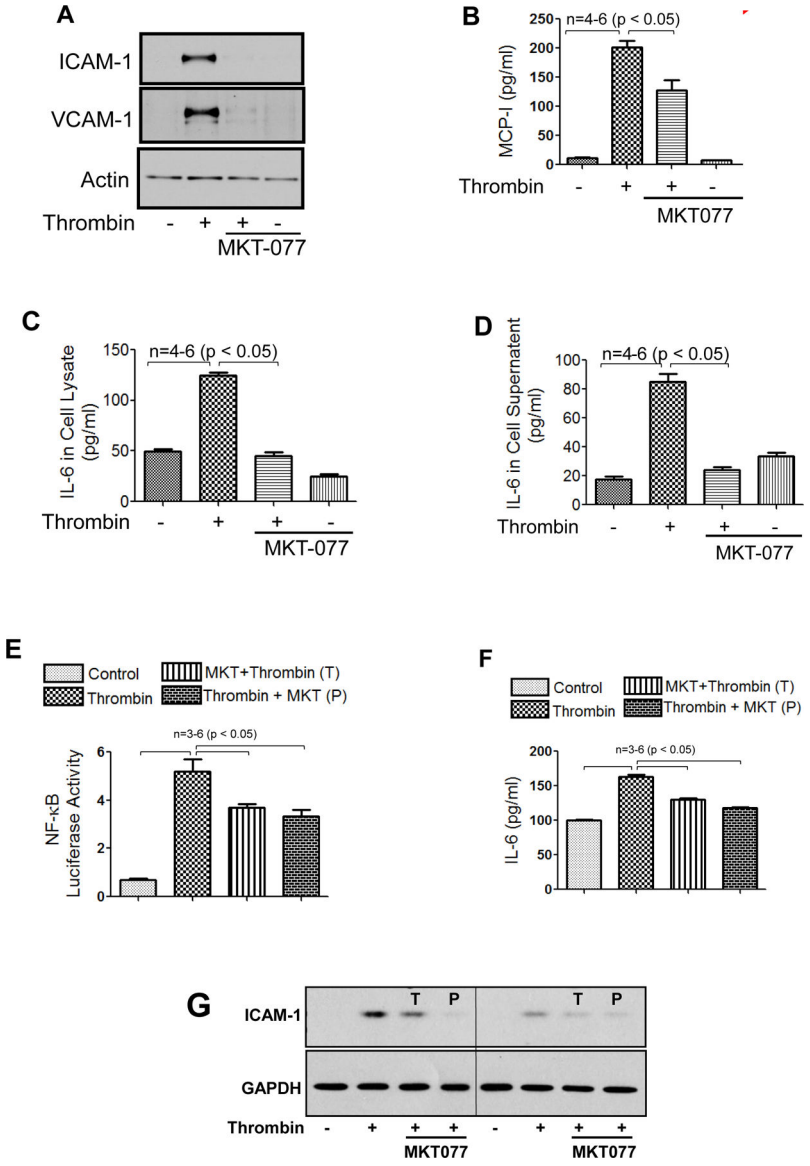

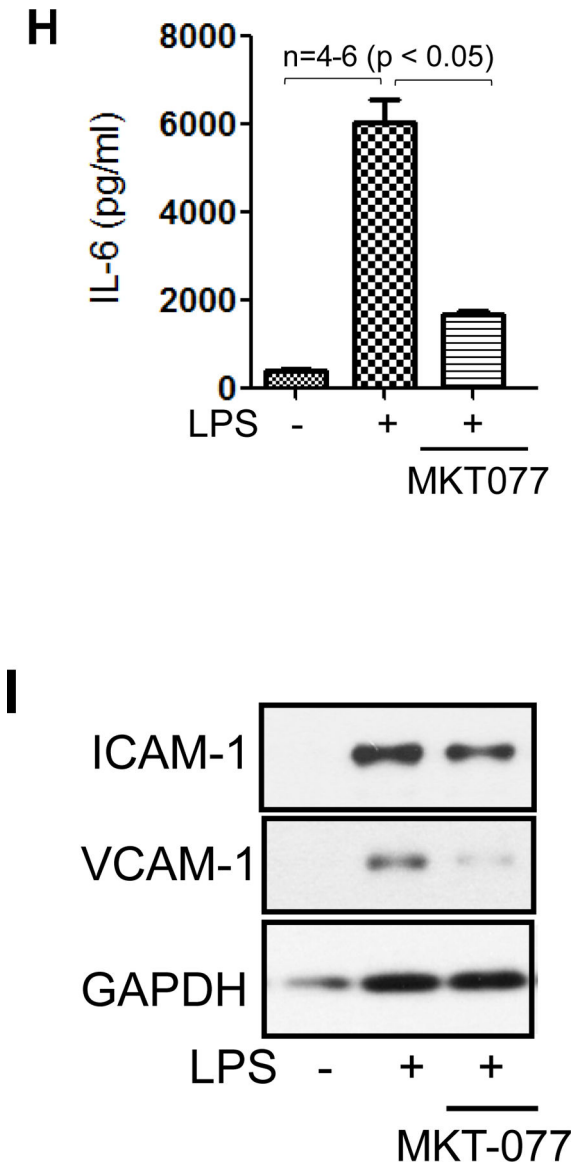

Figure 2. MKT-077 protects against thrombin and LPS-induced inflammatory responses.

(A–D) HPAEC were treated with 1μg/ml MKT-077(1 h) followed by thrombin treatment (5 U/ml) for 6 h. Total cell lysate was immunoblotted for ICAM-1, VCAM-1, MCP-1 and IL-6 and culture supernatants were analyzed for IL-6 and MCP-1 using ELISA. ***(E)*** HPAEC were transfected with NF-κB-LUC and pTKRLUC constructs by DEAE-dextran as described in Methods. Cells were then treated with 1μg/ml MKT-077(1 h) before or 1 h after thrombin treatment (5 U/ml) for 6 h and cell extracts were prepared and assayed for Firefly and Renilla luciferase activities. ***(F&G)*** luciferase lysates were immunoblotted for IL-6 using ELISA and for ICAM-1 using anti-ICAM-1 antibody. Anti-GAPDH antibody was used to monitor loading control. ***(H–I)*** HPAEC were treated with 1μg/ml MKT-077 (1 h) followed by LPS treatment (0.1μg/ml) for 6 h. Cell culture supernatants were analyzed for IL-6 using ELISA. Total cell lysates were immunoblotted for ICAM-1 and VCAM-1. Anti-GAPDH antibody was used to monitor loading control. The blot in 2I is cropped from a gel.

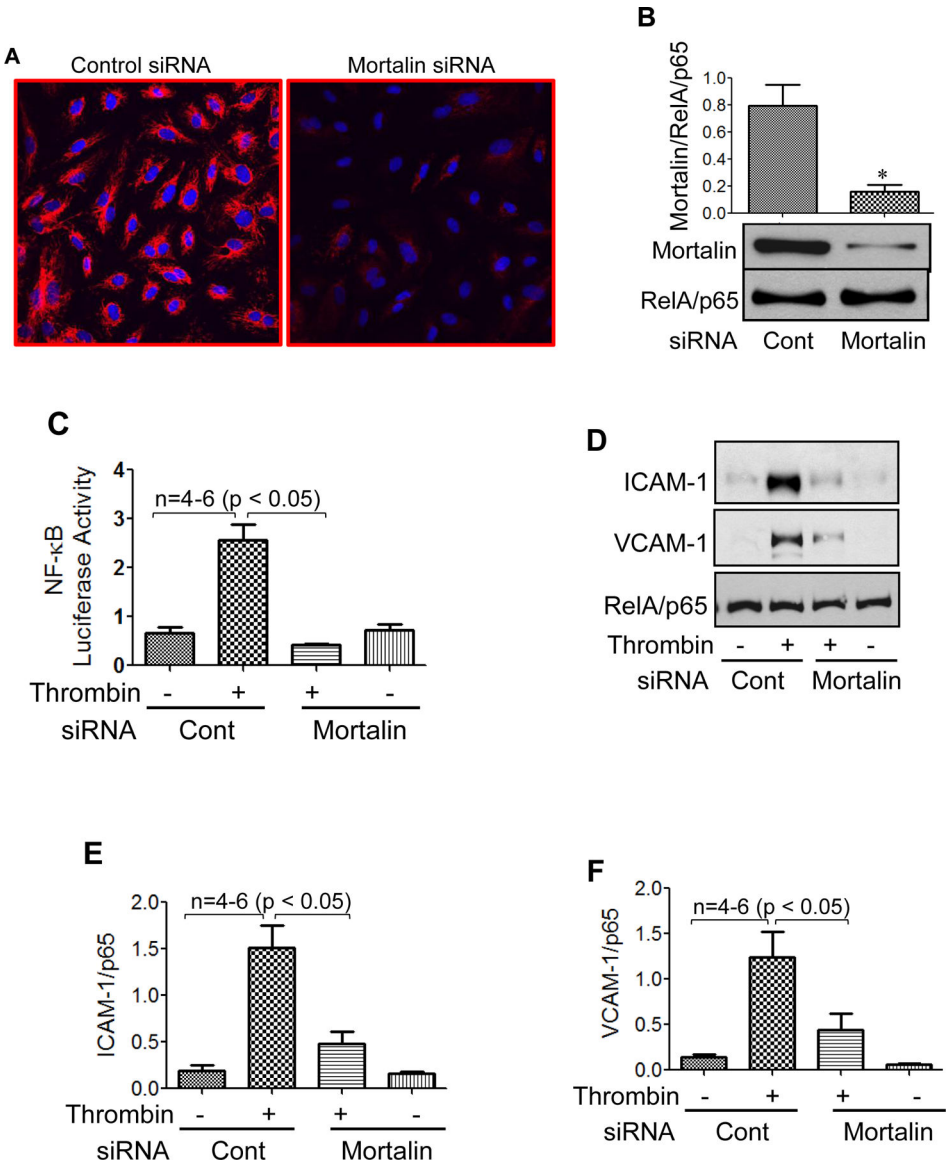

Figure 3. Mortalin knockdown attenuates thrombin-induced NF-κB reporter activity and mitigates inflammatory gene expression.

(A) HPAEC grown to confluence on 2% gelatin-coated coverslips were transfected with control siRNA or mortalin siRNA using DharmaFect1. After 24–36 h cells were fixed, permeabilized and stained with anti-mortalin antibody to visualize depletion of mortalin. ***(B)*** Total cell lysates were immunoblotted for mortalin levels using anti-mortalin antibody. ***(C-F)*** HPAEC were transfected with control siRNA or mortalin siRNA using DharmaFect1. Twenty four hours later cells were again transfected with NF-κB-LUC and pTKRLUC constructs by DEAE-dextran as described in Methods. Cells were then challenged with thrombin (5 U/ml) for 6 h. Cell extracts were prepared and assayed for Firefly and Renilla luciferase activities. Lysates were also immunoblotted for ICAM-1 and VCAM-1 using anti-ICAM-1 and anti-VCAM-1 antibody. Anti-RelA/p65 antibody was used as a loading control.

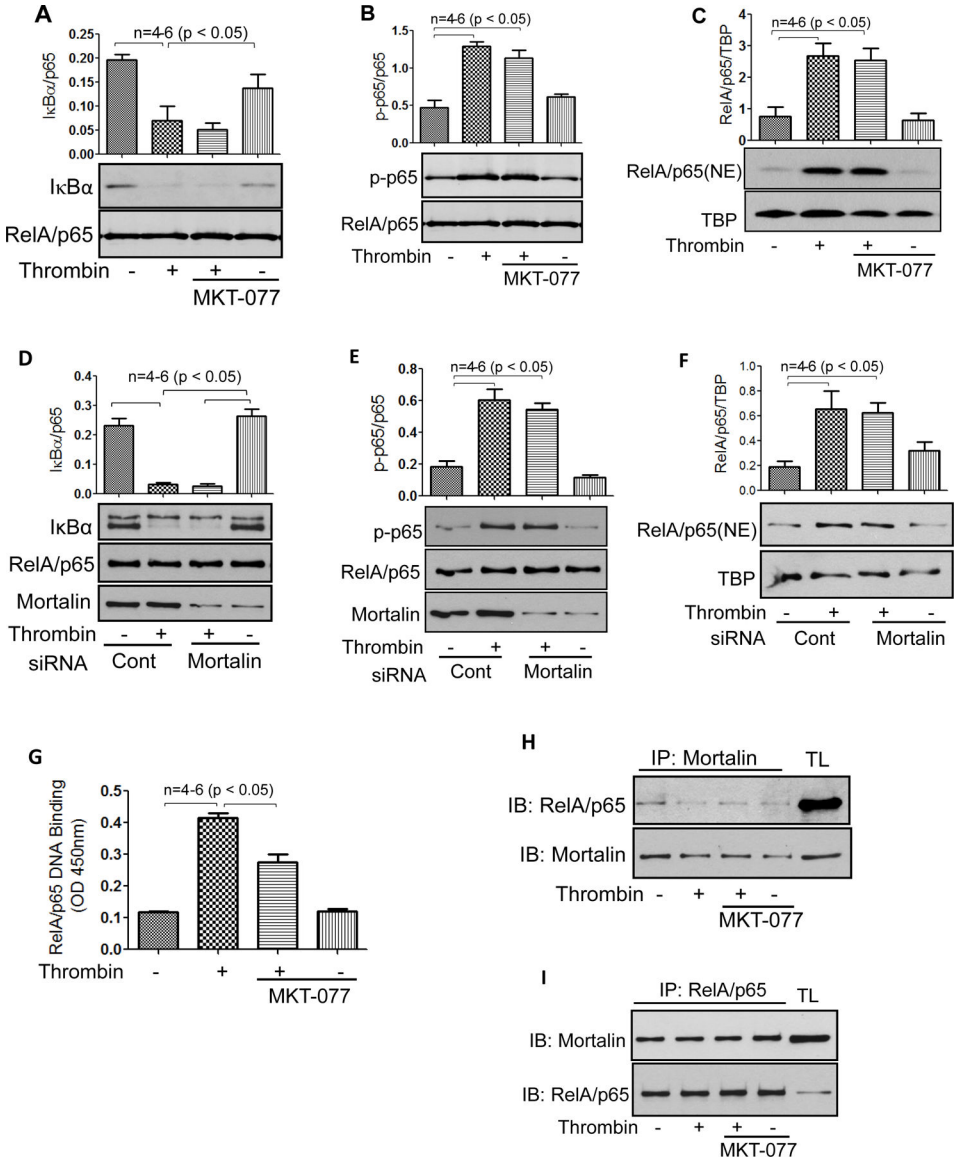

Figure 4. Mortalin regulates NF-κB signaling in EC.

(A&B) HPAEC grown to confluence were treated with 1μg/ml MKT-077 (1h) followed by thrombin treatment (5 U/ml) for 1 h. Total cell lysates were prepared and immunoblotted with anti- IκBα antibody or anti-phospho serine (Ser^{536}) antibody. Anti-RelA/p65 antibody was used to monitor loading. ***(C)*** HPAEC grown to confluence were treated with 1μg/ml MKT-077 (I h) followed by thrombin treatment (5 U/ml) for 1 h. Nuclear extracts (NE) were separated by SDS-PAGE and immunoblotted with anti-RelA/p65 antibody. Tata binding protein (TBP), a nuclear protein, was used as loading control for nuclear extracts. ***(D&E)*** HPAEC were transfected with control siRNA or mortalin siRNA using DharmaFect1. 24–36 hours later cells were treated with thrombin (5 U/ml) for 1 h. Total cell lysates were prepared and immunoblotted using anti- IκBα antibody, anti-phospho serine (Ser^{536}) antibody. Anti-RelA/p65 antibody was used to monitor loading. Mortalin antibody was used to monitor mortalin depletion. ***(F)*** HPAEC were transfected with control siRNA or mortalin

siRNA using DharmaFect1. 24–36 hours later cells were treated with thrombin (5 U/ml) for 1 h. NE were separated by SDS-PAGE and immunoblotted with anti-RelA/p65 antibody. TBP was used as loading control for nuclear extracts. ***(G)*** HPAEC were treated with 1μg/ml MKT-077 (I h) followed by thrombin treatment (5 U/ml) for 1 h. Nuclear extracts were prepared and assayed for DNA binding of RelA/p65 using Cayman's NF-κB (RelA/p65) Transcription Factor Assay Kit as described in Materials and Methods. The data are the means ±S.E. (n= 4–6 for each condition). ***(H&I)*** HPAEC were treated with 1μg/ml MKT-077 (1h) followed by thrombin treatment (5 U/ml) for 1 h. Total cell lysates were subjected to immunoprecipitation with an antibody to mortalin/GRP75 ***(H)*** or antibody to RelA/p65 ***(I).*** The immunoprecipitates were then immunoblotted with antibody to RelA/p65 or mortalin/GRP75 and vice versa. TL; total lysate.

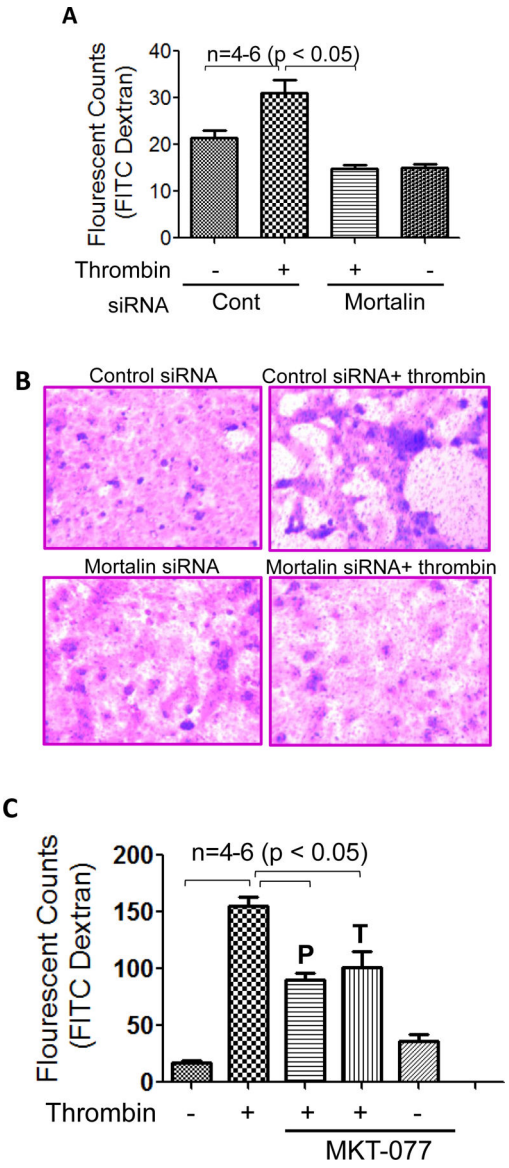

Figure 5. Mortalin regulates thrombin-induced endothelial permeability.

(A) HPAEC transfected with control-siRNA or mortalin-siRNA were seeded at 20,000 cells per transwell insert and cultured for 48 hours. Following this, the confluent monolayer was treated with thrombin (5 U/ml) for 30 minutes. FITC-Dextran permeability testing was done to check monolayer integrity. Permeation was stopped by removing the inserts from the wells. Media from the receiver tray was transferred to a 96 well opaque plate to measure fluorescence. Fluorescent intensities were quantified using a fluorescent plate reader with filters appropriate for 485 nm and 535 nm excitation and emission. The data are the means ± S.E. (n = 4–6 for each condition). ***(B)*** Following permeability testing the endothelial monolayers were stained for bright field imaging. ***(C)*** HPAEC were treated with 1μg/ml MKT-077 (1 h) before or 1 h after thrombin treatment (5 U/ml; 1 h). In vitro FITC dextran permeability assay was performed to monitor thrombin-induced endothelial permeability.

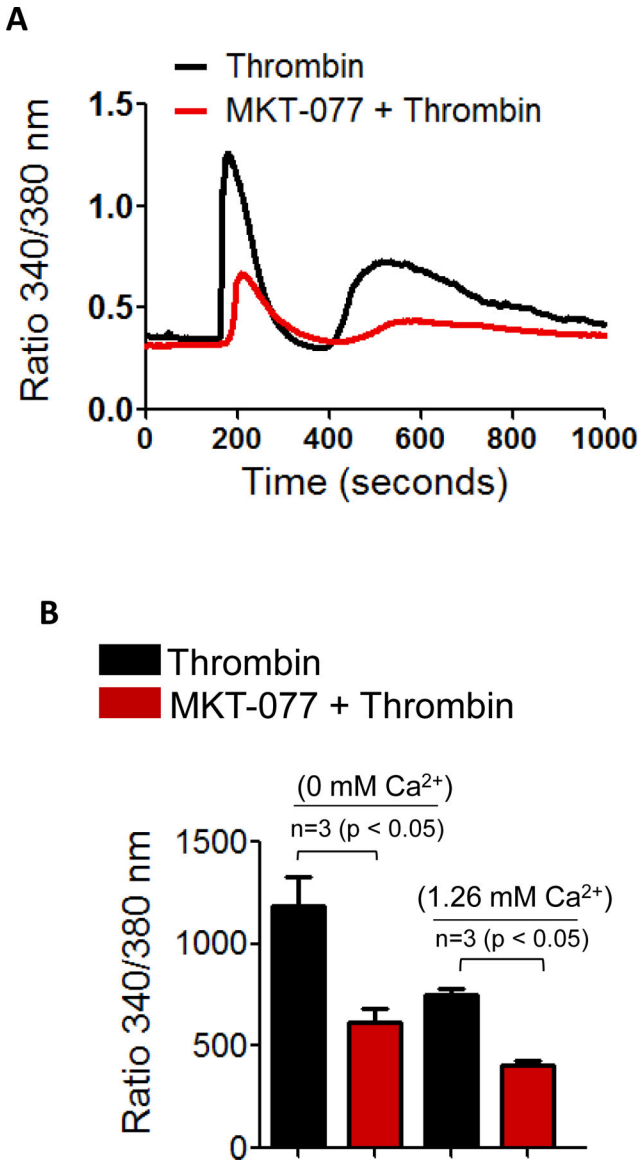

Figure 6. Mortalin regulates thrombin-induced Ca^{2+} release and entry in EC.

(***A&B***) HPAEC grown to confluence on 25 mm coverslips were left untreated or treated with 1 μg/ml of MKT-077 for 1 h. Cells were then loaded with Fura2-AM for 30 min and washed twice with Ca^{2+} free HBSS buffer and mounted on an inverted microscope. Calcium release from the intracellular stores was determined by perfusing Ca^{2+} free imaging buffer and stimulating cells with thrombin (2.5 U/ml). Store-operated Ca^{2+} entry was measured following addition of 1.26 mM Ca^{2+}. Fura-2 ratio (F-ratio 340/380) was calculated and analyzed with NIS-Element AR 3.0 Software.